Electronic Supplementary Material (ESI) for Materials Advances.

Additive Engineering for High-Performance P3HT:Non-fused Ring Electron Acceptor Organic Solar Cell

Dou Luo,[ad#] Lanqing Li[b#], Erjun Zhou,[c] Wai-Yeung Wong[d] and Aung Ko Ko Kyaw*[a]

[a] *Guangdong University Key Laboratory for Advanced Quantum Dot Displays and Lighting, Department of Electrical & Electronic Engineering, Southern University of Science and Technology, Shenzhen 518055, China.*

[b] *School of Biotechnology and Health Sciences, Wuyi University, Jiangmen 529020, China.*

[c] *National Center for Nanoscience and Technology, Beijing 100190, China.*

[d] *Department of Applied Biology and Chemical Technology and Research Institute for Smart Energy, The Hong Kong Polytechnic University, Hung Hom, Hong Kong, China.*

# These authors contribute equally to this work.

* Corresponding author, E-mail address: aung@sustech.edu.cn

1.1 Experimental Section

All manipulations involving air-sensitive reagents were performed under an inert atmosphere of dry nitrogen. Compounds 4,4-bis(2-ethylhexyl)-6-(tributylstannyl)-4H-cyclopenta[2,1-b:3,4-b']dithiophene-2-carbaldehyde **(2)** [1]was synthesized according to the method in the literature. All the other starting materials, unless otherwise specified, were purchased commercially and used as received without further purification.

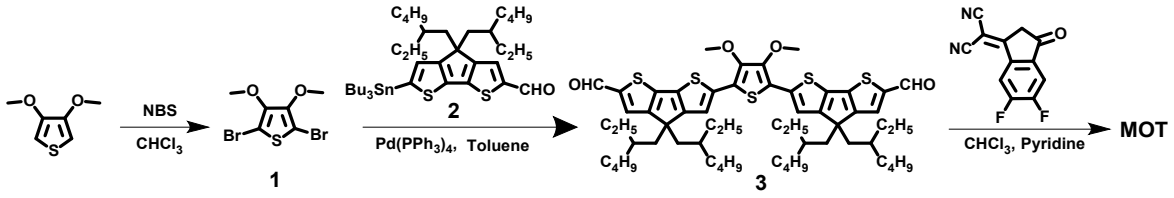

Scheme S1. Synthetic route of MOT.

Synthesis of 2,5-dibromo-3,4-dimethoxythiophene **(1)**

3, 4-dimethoxythiophene (1.5 g, 10.4 mmol) was added in 30 mL chloroform under nitrogen atmosphere. N-bromosuccinimide (4.25 g, 23.9 mmol) was then added dropwise in the solution and left stirring for another 4 h. Then the mixture was poured into water and extracted with CH_2Cl_2 for three times. The organic layer was washed with water and then dried over $MgSO_4$. After removal of solvent, the crude product was purified on a silica-gel column chromatography using petroleum ether as the eluent to afford colorless liquid (2.82 g, 90 %). ^{1}H NMR (400 MHz, $CDCl_3$, ppm): δ 3.91 (s, 6H). HRMS: calcd for $C_6H_6Br_2O_2S$, 301.98; found, 301.50 (100%).

Synthesis of 6,6'-(3,4-dimethoxythiophene-2,5-diyl)bis(4,4-bis(2-ethylhexyl)-4H cyclopenta[2,1-b:3,4-b']dithiophene-2-carbaldehyde) **(3)**

$Pd(PPh_3)_4$ (24.0 mg, 0.02 mmol) was added quickly to a mixture of compound **1** (100 mg, 0.30 mmol) and compound **2** (500 mg, 0.69 mmol) in toluene (30 mL) under nitrogen atmosphere. The reaction was heated at 110 °C for 24 h. After being cooled to room temperature, 50 mL of 2 mol/L KF solution was added and then the resulting mixture continued stirring for 20 min. After being filtered, the filtrate was treated with water and extracted with CH_2Cl_2. The organic layer was separated, dried over anhydrous $MgSO_4$ and concentrated under reduced pressure. The residue was subjected to column chromatography over silica gel using petroleum ether/CH_2Cl_2

as eluent to afford a dark red solid (302.1 mg, 81%). ^{1}H NMR (400 MHz, $CDCl_3$, ppm): δ 9.83 (s, 2H), 7.56-7.55 (m, 2H), 7.11-7.09 (m, 2H), 4.05-4.01 (m, 6H), 1.95-1.87 (m, 8H), 1.56-1.54 (m, 4H), 1.00-0.92 (m, 32H), 0.77-0.74 (m, 12H), 0.65-0.60 (m, 12H). HRMS: calcd for $C_{58}H_{80}O_4S_5$, 1001.57; found, 1001.3.

Synthesis of 2,2'-((2Z,2'Z)-(((3,4-dimethoxythiophene-2,5-diyl)bis(4,4-bis(2-ethylhexyl)-4H-cyclopenta[2,1-b:3,4-b']dithiophene-6,2-diyl))bis(methanylylidene))bis(5,6-difluoro-3-oxo-2,3-dihydro-1H-indene-2,1-diylidene))dimalononitrile **(MOT)**

2-(5,6-difluoro-3-oxo-2,3-dihydro-1H-inden-1-ylidene)malononitrile (70 mg, 0.299 mmol) was added to a solution of compound **3** (100 mg, 0.099 mmol) in $CHCl_3$ (30 mL) under nitrogen atmosphere. Then 1 mL pyridine was injected into the solution. The mixture was stirred at 60 °C for 12 h. After being cooled to room temperature, the mixture was poured into water and extracted with CH_2Cl_2. The organic layer was washed with water and then dried over $MgSO_4$. After removal of solvent, the crude product was purified on a silica-gel column chromatography using CH_2Cl_2 as the eluent. **MOT** was obtained as a black solid (106.8 mg, 75%). ^{1}H NMR (400 MHz, $CDCl_3$, ppm): δ 8.88 (s, 2H), 8.54-8.49 (m, 2H), 7.67-7.63 (m, 4H), 7.19-7.18 (m, 2H), 4.08-4.06 (m, 6H), 2.02-1.91 (m, 8H), 1.01-0.93 (m, 36H), 0.76-0.73 (m, 12H), 0.67-0.62 (m, 12H). ^{13}C NMR (101 MHz, $CDCl_3$, ppm): δ 186.80, 182.56, 178.17, 166.48, 160.16, 159.22, 156.06, 153.37, 148.26, 143.08, 139.62, 138.74, 138.53, 137.93, 137.16, 135.10, 120.66, 119.74, 118.97, 115.52, 115.39, 68.15, 61.00, 54.56, 43.95, 36.13, 34.66, 29.13, 27.95, 23.48, 14.77, 11.27. HRMS: [M+H] calcd for $C_{82}H_{84}F_4N_4O_4S_5$ 1425.89; found, 1425.12. Anal. Calcd. for $C_{82}H_{84}F_4N_4O_4S_5$: C 69.07, H 5.94, N 3.93, S 11.24; found: C 69.25, H 6.01, N 3.86, S 11.28.

1.1 General Measurement and Characterization

^{1}H NMR and ^{13}C NMR spectra was recorded on Bruker Ascend 400 MHz spectrometer, respectively. High-resolution mass spectra were obtained with Thermo Scientific™ Q-Exactive. Elemental analyses (EAs) of compounds were performed on Vario EL cube with CHNS pattern in Fudan University (Shanghai, China).

UV-Vis-NIR absorption spectra were recorded on a Shimadzu UV-3600 UV-Vis-NIR spectrometer. The PL spectra were measured by using a HORIBA LabRAM HR Evolution spectrometer and 583 nm as an excitation source. The neat P3HT, MOT and P3HT:MOT (1-CN, 1-MN, 1-PN) were spin-cast on quartz glass from 15 mg mL^{-1} $CHCl_3$ solution (total concentration) at a speed of 2000 rpm.

Cyclic voltammetry (CV) was measured on a CHI630E Electrochemical Workstation equipped with a glass carbon working electrode, a platinum wire counter electrode, and an Ag/AgCl reference electrode. The measurements were carried out in dry dichloromethane with tetrabutylammonium hexafluorophosphate (0.1 mol L^{-1}) as the supporting electrolyte under a nitrogen atmosphere at a scan rate of 100 mV s^{-1}. The potential of Ag/AgCl reference electrode was internally calibrated by using the ferrocene/ferrocenium redox couple (Fc/Fc^{+}). Atomic force microscopy (AFM) measurements were carried out using a NanoMan VS microscope in the tapping mode. TEM images were obtained from a JEM-2100F instrument. The time-resolved PL (TRPL) measurements were performed with an Edinburgh Instruments spectrometer (FLS980), the active layer film was excited by a 532 nm pulsed laser.

1.2 Femtosecond (fs) Transient Absorption (TA) Spectroscopy Characterization

For femtosecond transient absorption spectroscopy, the fundamental output from Yb:KGW laser (1030 nm, 220 fs Gaussian fit, 100 kHz, Light Conversion Ltd) was separated to two light beam. One was introduced to NOPA (ORPHEUS-N, Light Conversion Ltd) to produce a certain wavelength for pump beam, the other was focused onto a YAG plate to generate white light continuum as probe beam. The pump and probe overlapped on the sample at a small angle less than 10°. The transmitted probe light from sample was collected by a linear CCD array. A pump pulse of 800 nm (below 5 μJ/cm^2) was employed to excite only acceptors and after a certain delay time, probed the relative transmittance change (ΔA) using a white-light continuum. The primary absorption peaks for different acceptors and donors are well separated in the spectral domain,

therefore, both the spectral and temporal characteristics of hole transfer dynamics can be extracted.

1.3 Contact angle measurements

The contact angle tests were performed on a Dataphysics OCA40 Micro surface contact angle analyzer. The surface energy of the polymers was characterized and calculated by the contact angles of the two probe liquids with the Wu model.[2,3]

$$\frac{4\gamma_{\text{water}}^{\text{d}}\gamma_{\text{s}}^{\text{d}}}{\gamma_{\text{water}}^{\text{d}} + \gamma_{\text{s}}^{\text{d}}} + \frac{4\gamma_{\text{water}}^{\text{p}}\gamma_{\text{s}}^{\text{p}}}{\gamma_{\text{water}}^{\text{p}} + \gamma_{\text{s}}^{\text{p}}} = \gamma_{\text{water}}(1+\cos\theta_{\text{water}})$$

$$\frac{4\gamma_{\text{oil}}^{\text{d}}\gamma_{\text{s}}^{\text{d}}}{\gamma_{\text{oil}}^{\text{d}} + \gamma_{\text{s}}^{\text{d}}} + \frac{4\gamma_{\text{oil}}^{\text{p}}\gamma_{\text{s}}^{\text{p}}}{\gamma_{\text{oil}}^{\text{p}} + \gamma_{\text{s}}^{\text{p}}} = \gamma_{\text{oil}}(1+\cos\theta_{\text{oil}})$$

where γ_{s} is the total surface energy of acceptors and polymers, and $\gamma_{\text{s}}^{\text{d}}$ and $\gamma_{\text{s}}^{\text{p}}$ are the dispersion and polar components of γ_{s}, the values of $\gamma_{\text{water}}^{\text{d}}$, $\gamma_{\text{water}}^{\text{p}}$, $\gamma_{\text{oil}}^{\text{d}}$, $\gamma_{\text{oil}}^{\text{p}}$ could be could be found from the literature and θ is the droplet contact angle between sample and probe liquid.

1.4 Fabrication of organic solar cells

All devices were fabricated based on conventional structure: ITO/PEDOT:PSS/active layer/PDINN/Ag. ITO-coated glass substrates were cleaned by sonification in acetone, detergent, deionized water, and isopropyl alcohol and dried in a nitrogen stream. The pre-cleaned ITO substrate was coated with PEDOT: PSS (filtered through a 0.45 μm PES filter) by spin-coating (4000 rpm. for 30 s, thickness of ~30 nm) and then baked at 150 °C on a hotplate for 15 min in air. The PEDOT:PSS-coated ITO substrates were transferred into a N_2-filled glove box for subsequent steps. The P3HT:MOT (1:1.2 weight ratio) active layer prepared by spin-casting chloroform solution at 2600 rpm for 30 s. The total concentration was 17 mg mL^{-1} with 0.5% (v:v 99.5:0.5) 1-chloronaphthalene (CN), 1-phenylnaphthalene (1-PN) or 1-methoxynaphthalene (1-MN) as the additives. The thickness is approximately 100 nm as measured by the profilometer. Before spin-coating the electron transporting layer, all active layers were thermally annealed at

130 °C for 50 min. Finally, 5 nm of the perylene diimide functionalized (PDINN)[4] (1 mg mL^{-1} in methanol) was spin-coated at 3000 rpm for 30 s on the active layer followed by the deposition of 100 nm Ag cathode under a under high vacuum (< 2 $\times 10^{-4}$ Pa). All the active devices area were 0.056 cm^2 through a shadow mask. The current density–voltage (*J–V*) curves were measured using Keithley 2400 source meter under 1 sun (AM 1.5 G spectrum) generated from a class solar simulator (Japan, SAN-EI, XES-40S1). The external quantum efficiency (EQE) spectra were measured using a Solar Cell Spectral Response Measurement System QE-R3011 (Enlitech Co., Ltd.). The light intensity at each wavelength was calibrated using a standard single crystal Si photovoltaic cell.

1.5 Fabrication of single-carrier devices

Single-carrier device (ITO/PEDOT:PSS(40 nm)/active layer/MoO_3(10 nm)/Ag) and (ITO/ZnO(40 nm)/[5]active layer/PDINN/Ag) were fabricated to measure hole and electron mobility of the P3HT:MOT blend films. The active layers comprising P3HT:MOT were spin-cast from chloroform solution at 2600 rpm for 30 s (total concentration, 17 mg mL^{-1}). The thickness is approximately 100 nm as measured by the profilometer. The as-cast pure films were spin-cast from chloroform solution (total concentration, 12 mg mL^{-1}) at 1200 rpm for 30 s. The thickness is approximately 100 nm.

The mobility μ was derived from the SCLC model which is described by the equation $J = (9/8)\varepsilon_0\varepsilon_r\mu(V^2/d^3)$,[6] where J is the current, ε_0 the permittivity of free space, ε_r the relative permittivity of the material, d the thickness of the active layers, and V the effective voltage.

1.6 Supporting Figures

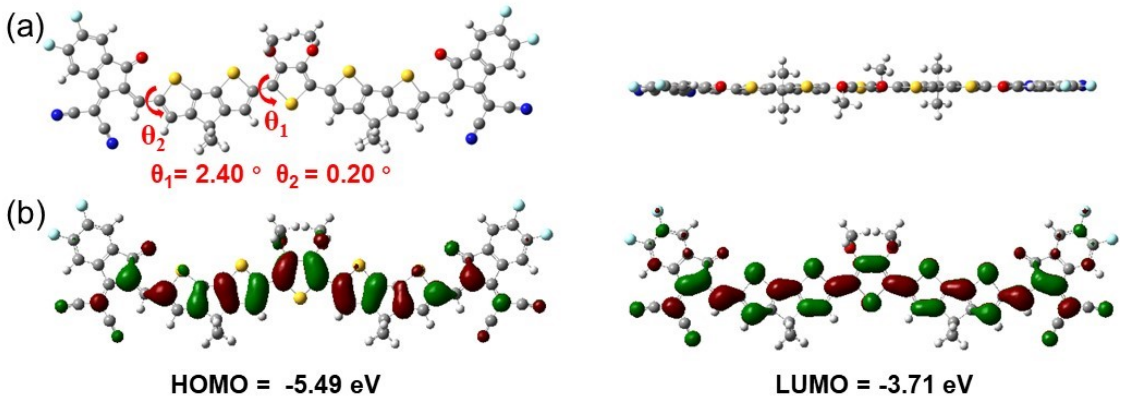

Fig. S1 Representative dihedral angles and spatial structure models and HOMO/LUMO levels of MOT calculated by Gaussian 09 with density function theory (DFT) at the level of B3LYP/6-31G. The alkyl chains were replaced with methyl groups.

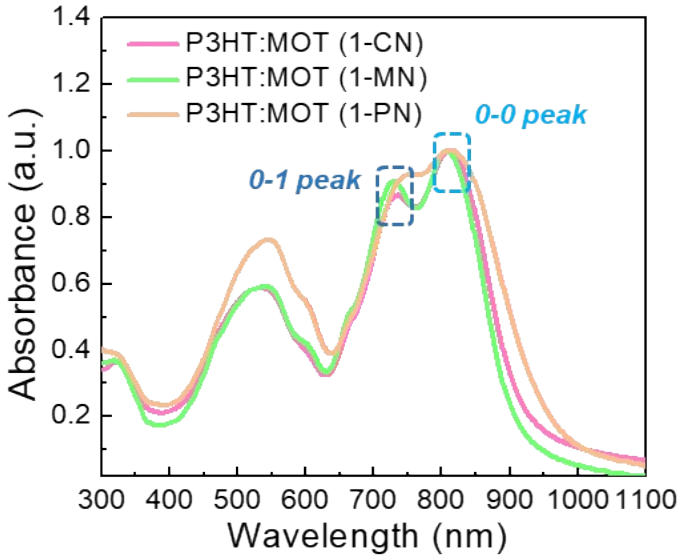

Fig. S2 Normalized UV-vis absorption spectra of P3HT:MOT with different additives as cast film.

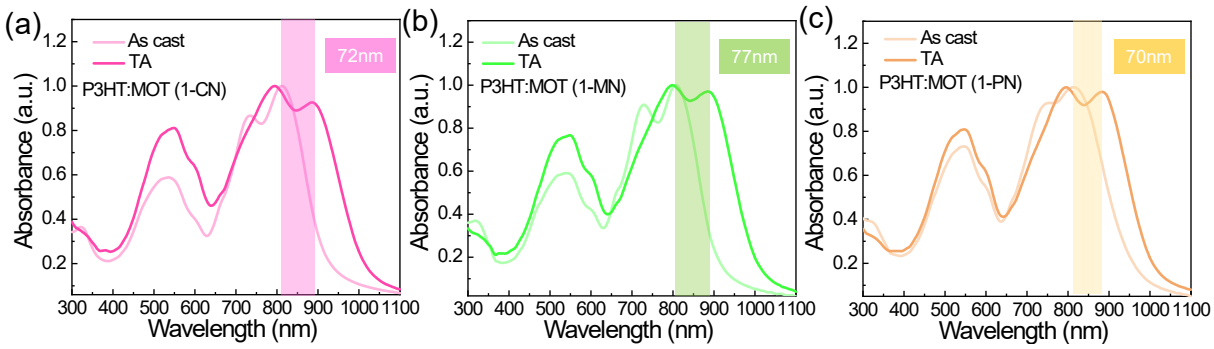

Fig. S3 Normalized UV-vis absorption spectra of P3HT:MOT as cast and thermal annealing films with (a) 1-CN, (b) 1-MN and (c) 1-PN additive.

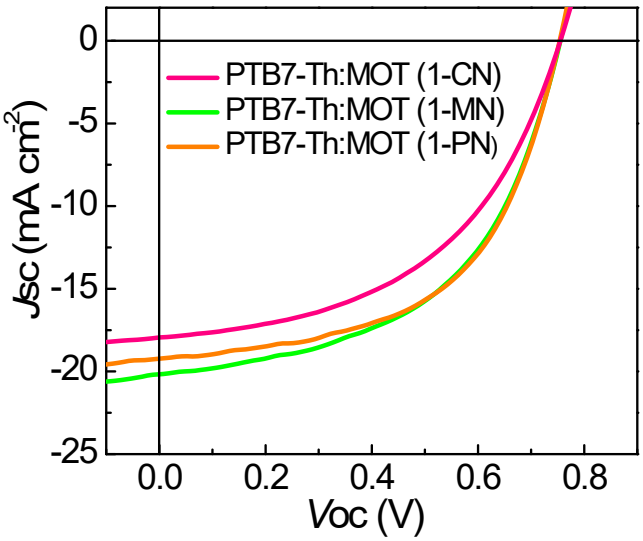

Fig. S4 *J*–*V* characteristics of the OSCs based on PTB7-Th:MOT under AM1.5G illumination (100 mW cm^{-2}).

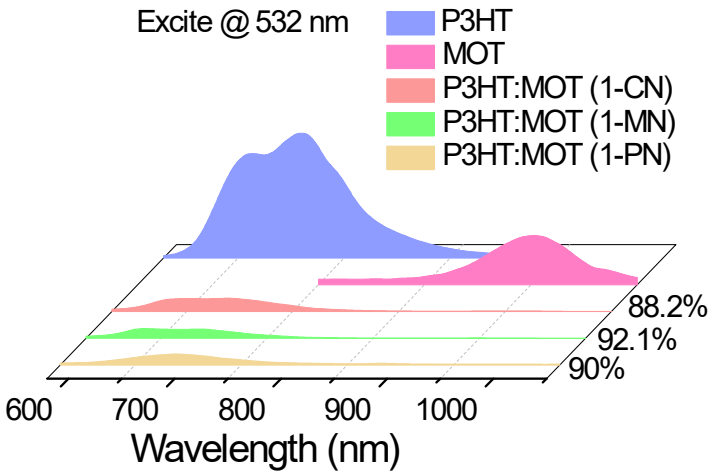

Fig. S5 PL spectra of pure P3HT, MOT and P3HT:MOT blend films under 532 nm light excitation.

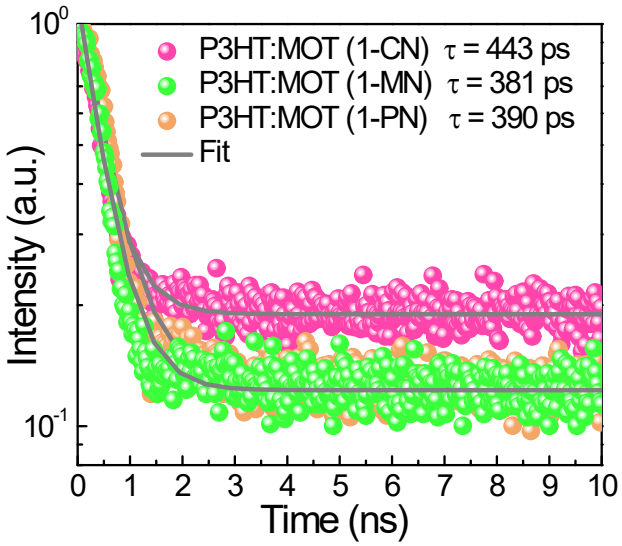

Fig. S6 TRPL decay spectra of P3HT:MOT blend films with different additives.

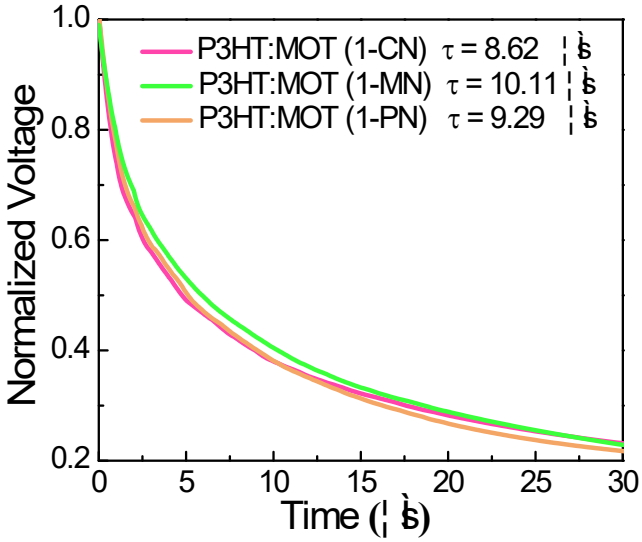

Fig. S7 Transient photovoltage (TPV) measurements of P3HT:MOT-based devices.

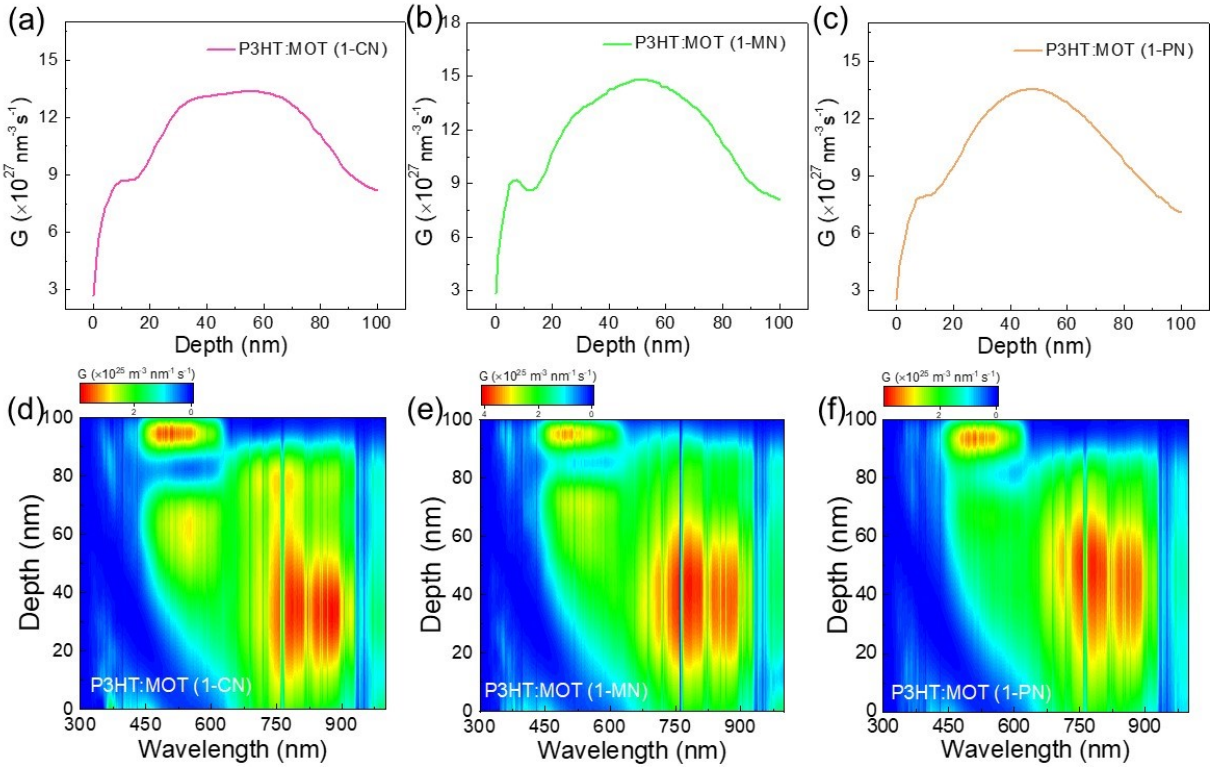

Fig. S8 (a-c) Film-depth-dependent exciton generation rates as obtained by integration of along the wavelength direction. (d-f) The simulated exciton generation rates distributions along with film depth direction for devices.

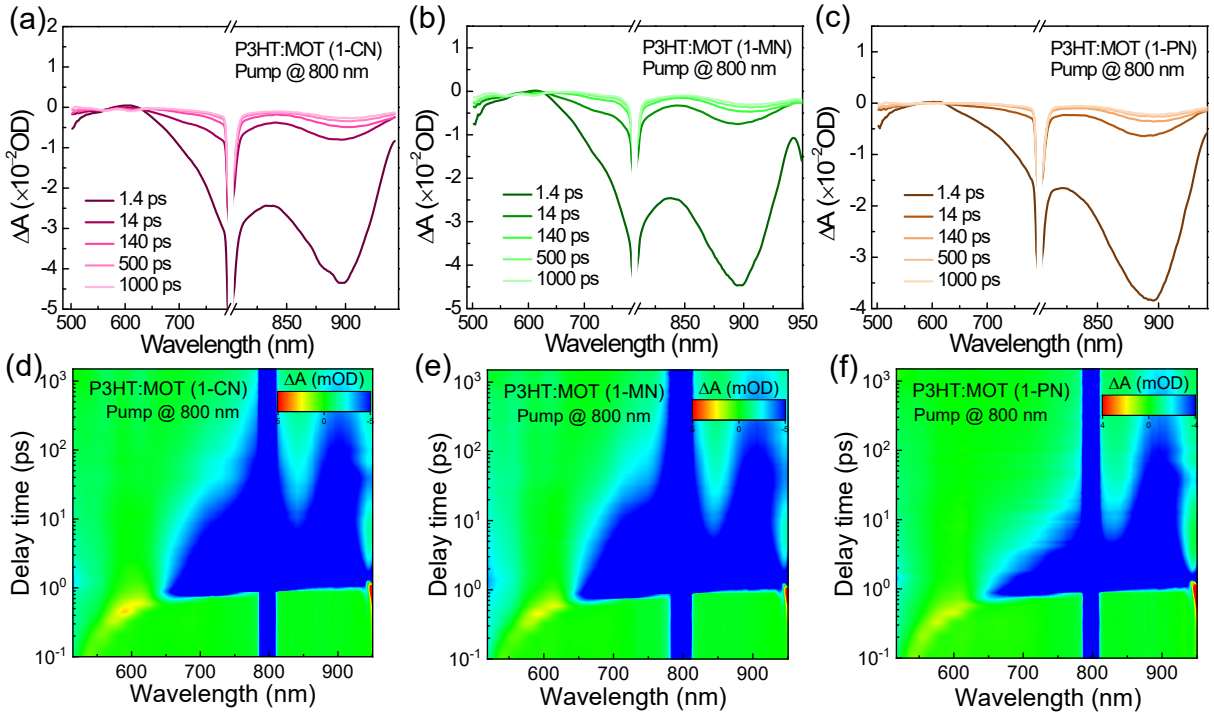

Fig. S9 TA spectra of P3HT:MOT films at indicated delay times under 800 nm excitation with (a) 1-CN (b) 1-MN and (c) 1-PN as additive, respectively. (d-f) Representative color plot of TA spectra of P3HT:MOT films with different additives.

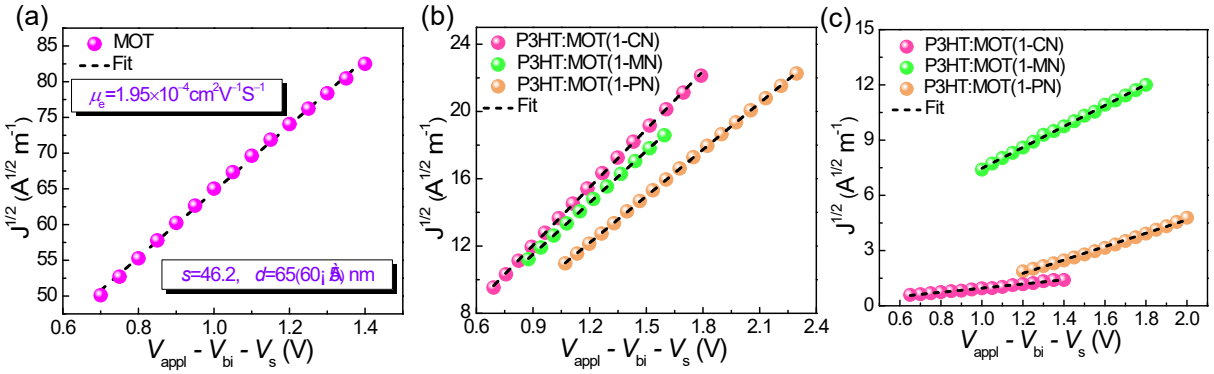

Fig. S10 (a) The $J^{1/2}$–V characteristics of the electron-only device of MOT. The $J^{1/2}$–V characteristics of the hole-only (b) and electron-only (c) devices based on the blend films P3HT:MOT.

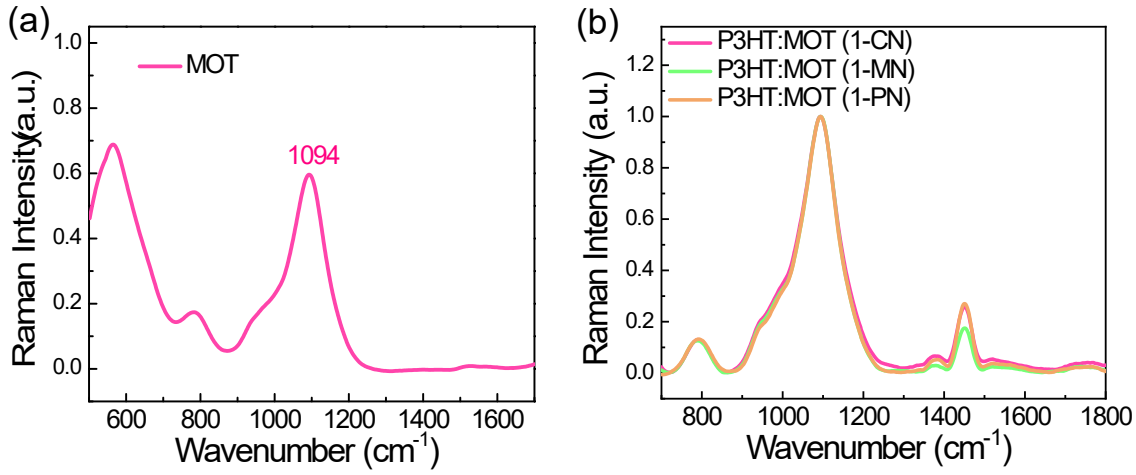

Fig. S11 Raman spectra of (a) pure MOT and (b) P3HT:MOT blend films under 532 nm laser excitation.

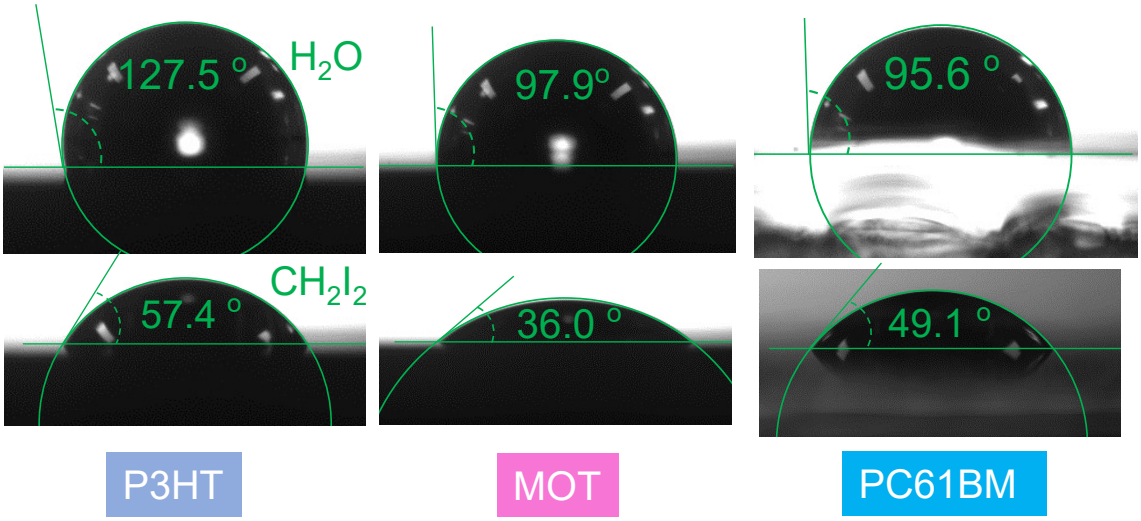

Fig. S12 Contact angles of water and diiodomethane droplets on the P3HT, MOT, PC61BM pristine films.

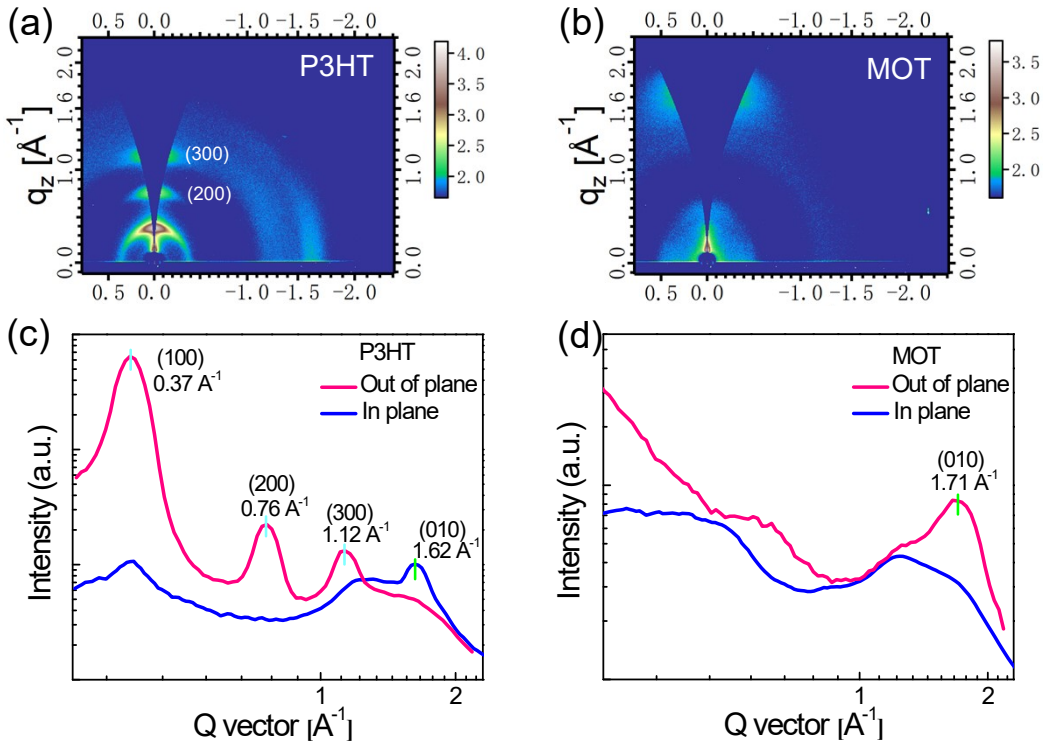

Fig. S13 GIWAXS patterns of (a) P3HT and (b) MOT neat films. out-of-plane and in-plane line-cut profiles of (c) P3HT and (d) MOT films.

1.7 Supporting Tables

Table S1 Photovoltaic parameters of OSCs based on P3HT:MOT blended films with different additives without thermal annealing.

Additive	V_{oc} (V)	J_{sc} (mA cm^{-2})	***FF***(%)	PCE (%)
1-CN	0.672	12.35	53.5	4.44
1-MN	0.671	13.68	56.7	5.20
1-PN	0.671	12.50	54.1	4.53

Table S2 Photovoltaic parameters of OSCs based on PTB7-Th:MOT blended films with different additives.

Additive	V_{oc} (V)	J_{sc} (mA cm^{-2})	***FF***(%)	PCE (%)
1-CN	0.754	17.9	50.42	6.80
1-MN	0.754	20.1	53.03	8.03
1-PN	0.753	19.1	54.2	7.79

Table S3 Detailed parameters of TA spectra, the electron transfer kinetics (excited at 500 nm and prob at 547 nm) were fitted by a biexponential function: $i = A_1 \exp(-t/\tau_1) + A_2 \exp(-t/\tau_2)$, with two lifetimes of τ_1 and τ_2 and pre-factors of A_1 and A_2.

Blend film	A_1	τ_1 (ps)	A_2	τ_2 (ps)	τ_m (ps)[a)]
P3HT:MOT (1-CN)	0.93	0.48	0.07	12.54	8.47
P3HT:MOT (1-MN)	0.92	0.46	0.08	10.07	6.80
P3HT:MOT (1-PN)	0.93	0.49	0.07	12.21	8.12

[a)] The average lifetime values were extracted by a biexponential function fit and calculated according to the equation: $\tau_m = \Sigma i\ Ai\tau i / \Sigma i\ Ai$.

Table S4 Hole and electron mobility in single-carrier devices for pure MOT film and for the P3HT:MOT blend films with different additives.

Blends film	μ_h (cm^2 V^{-1} s^{-1})	μ_e (cm^2 V^{-1} s^{-1})	μ_h / μ_e ratio
MOT	/	1.95×10^{-4}	
P3HT:MOT (1-CN)	3.2×10^{-5}	0.30×10^{-5}	10.66
P3HT:MOT (1-MN)	2.54×10^{-5}	0.78×10^{-5}	3.25
P3HT:MOT (1-PN)	2.07×10^{-5}	0.32×10^{-5}	6.46

Table S5 The contact angles and surface tension parameters of the pure and blend films.

Pristine film	θ_{water} (deg)	θ_{DIM} (deg)	γ^d (mN/m)	γ^p (mN/m)	Surface tension (mN/m)	χ
P3HT	127.5	57.4	20.83	0.35	21.18	–
$PC_{61}BM$	95.6	49.1	32.96	3.52	36.49	2.06 *K*
MOT	97.9	36.0	40.36	1.59	41.95	3.51 *K*
P3HT:MOT (1-CN)	109.1	48.3	32.58	0.01	32.59	
P3HT:MOT (1-MN)	106.4	54.7	33.29	0.01	33.30	
P3HT:MOT (1-PN)	103.7	58.2	30.10	1.27	31.37	

γ^d and γ^p represent the surface free energy (γ) generated from the dispersion forces and the polar forces, respectively. Surface energy (γ) = $\gamma^d + \gamma^p$

1.8 ^{1}H NMR, ^{13}C NMR and HRMS Spectra of MOT

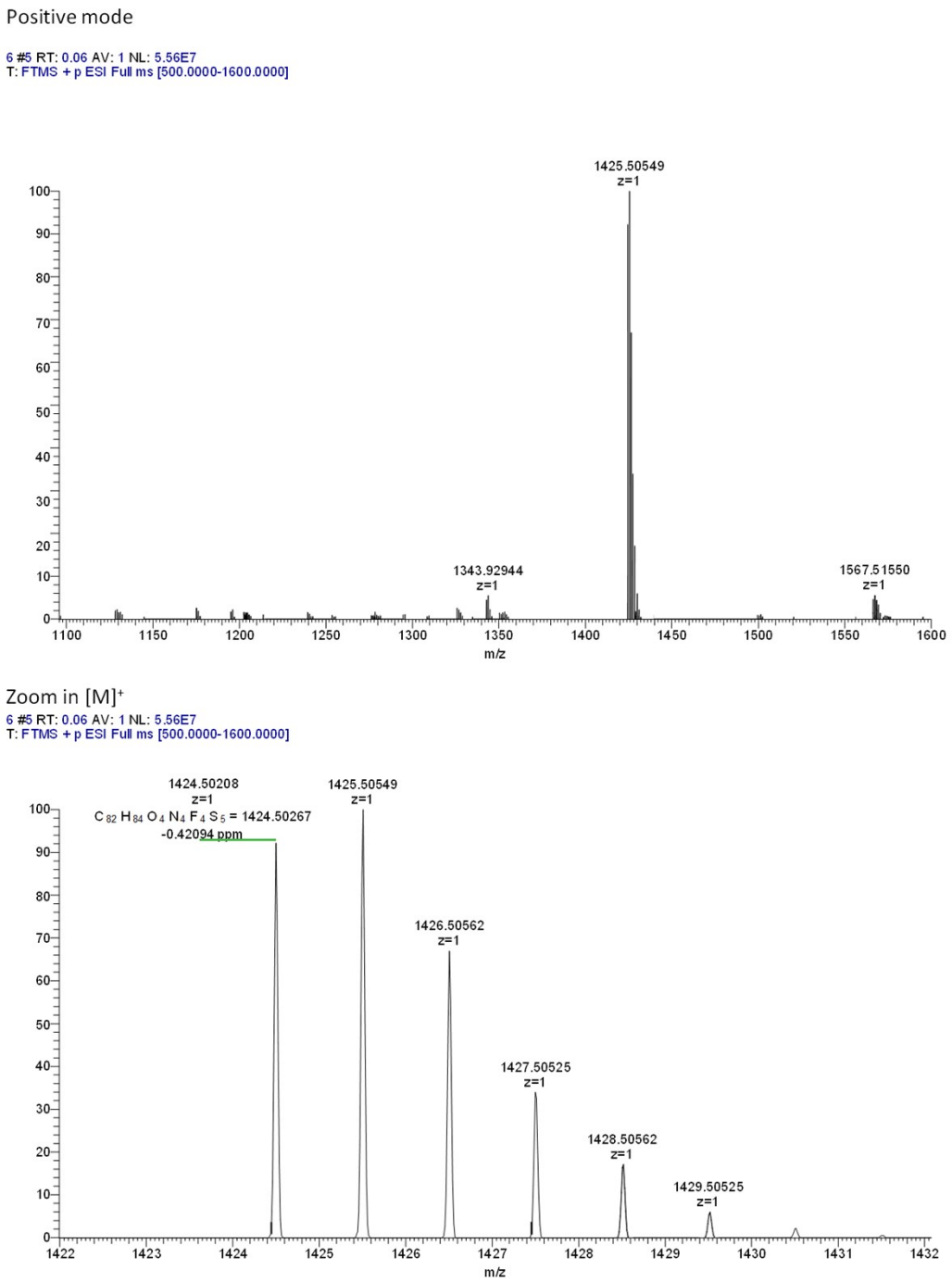

Fig. S14 HRMS of MOT.

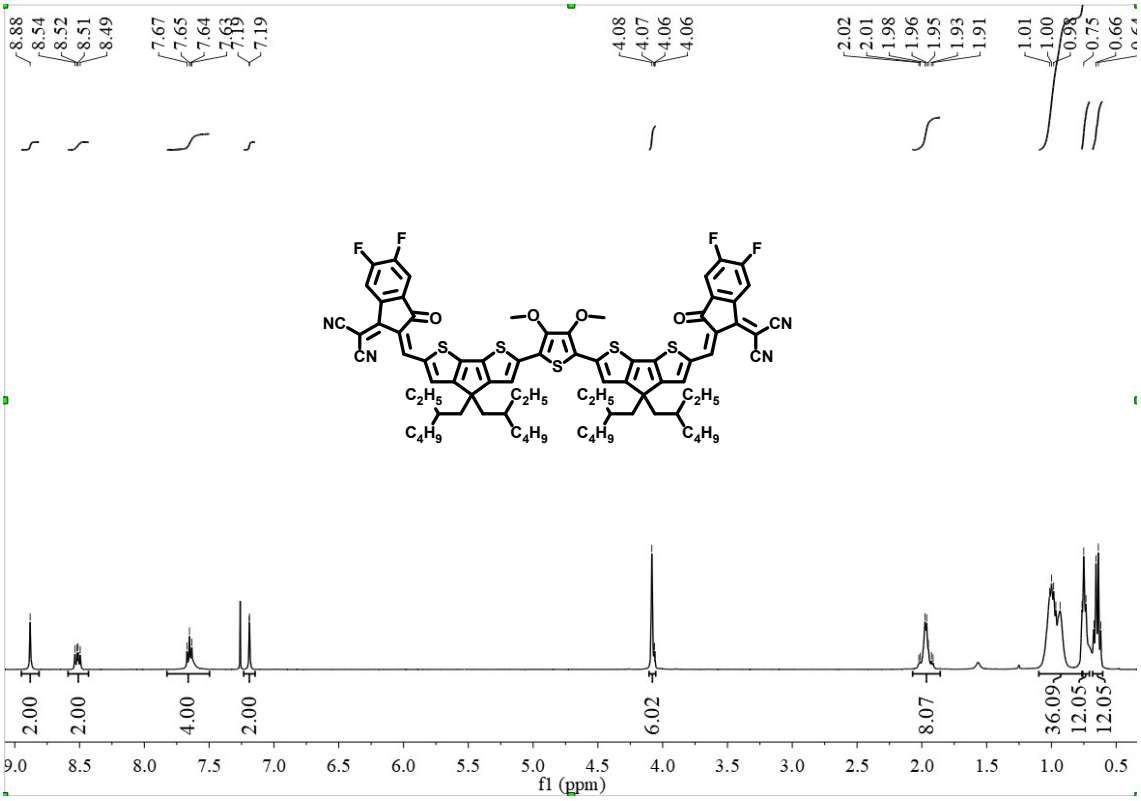

Fig. S15 ^{1}H NMR spectrum of MOT ($CDCl_3$, 400 MHz)

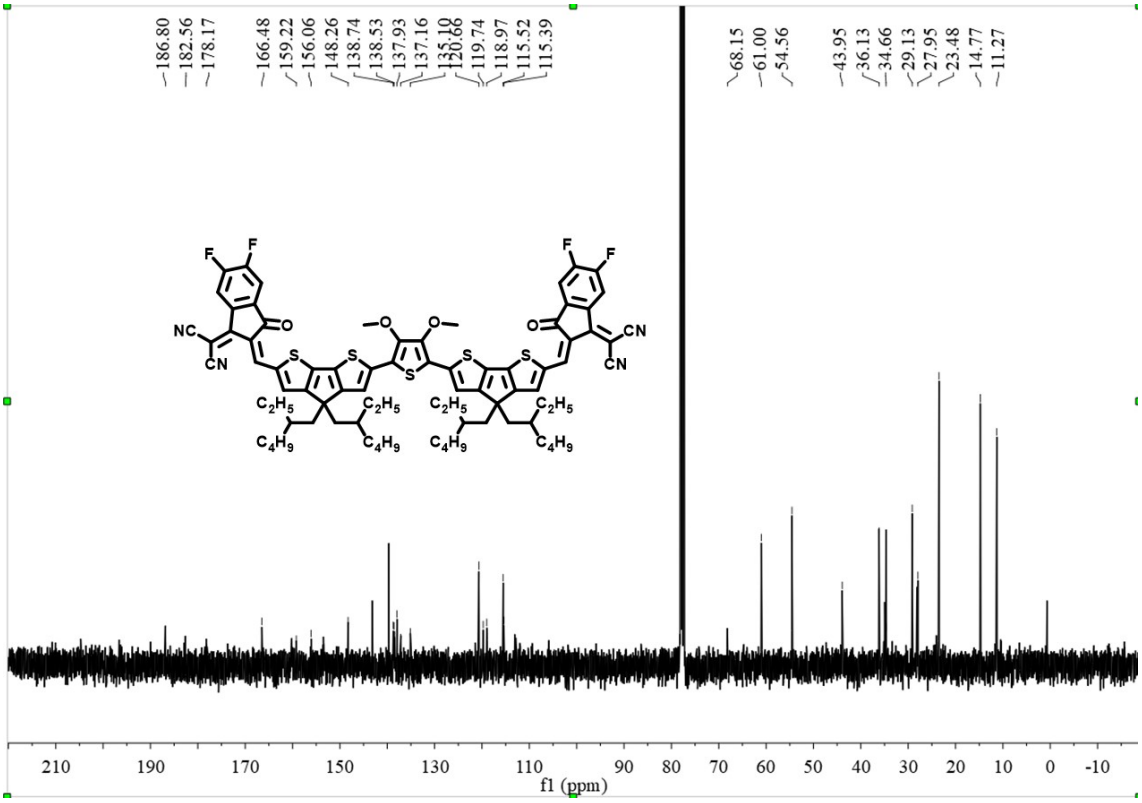

Fig. S16 ^{13}C NMR spectrum of MOT ($CDCl_3$, 400 MHz)

Reference

[1] Luo, D.; Li, L,, Shi, Y.; Zhang, J.; Wang, K.; Guo, X.; Kyaw, A. K. K. *J. Mater. Chem. A* **2021**, *9*, 14948.

[2] Wu, S. *J Adhes*. **1973**, *5*, 39-55.

[3] Comyn, J.; *Int J Adhesion Adhes*. **1992**, *12*, 145-149.

[4] Yao, J.; Qiu, B.; Zhang, Z.-G.; Xue, L.; Wang, R.; Zhang, C.; Chen, S.; Zhou, Q.; Sun, C.; Yang, C.; Xiao, M.; Meng, L.; Li Y. *Nat. Commun.* **2020**, *11*, 2726.

[5] Sun, Y.; Seo, J. H.; Takacs, C. J.; Seifter, J.; Heeger, A. J. *Adv*. *Mater*. **2011**, *23*, 1679-1683.

[6] Malliaras, G. G.; Salem, J. R.; Brock, P. J.; Scott, C. *Phys. Rev. B*. **1998**, *58*, 13411.